Bioconjugate Chemistry

pubs.acs.org/bc

Communication

# Human CD47-Derived Cyclic Peptides Enhance Engulfment of mAb-Targeted Melanoma by Primary Macrophages

AbdelAziz R. Jalil, Jason C. Andrechak, Brandon H. Hayes, David M. Chenoweth, and Dennis E. Discher*

Cite This: https://doi.org/10.1021/acs.bioconjchem.2c00020

Read Online

ACCESS | Metrics & More | Article Recommendations | Supporting Information



**ABSTRACT:** CD47 on healthy cells, cancer cells, and even engineered particles can inhibit phagocytic clearance by binding SIRP$\alpha$ on macrophages. To mimic and modulate this interaction with peptides that could be used as soluble antagonists or potentially as bioconjugates to surfaces, we made cyclic "nano-Self" peptides based on the key interaction loop of human CD47. Melanoma cells were studied as a standard preclinical cancer model and were antibody-opsonized to adhere to and activate engulfment by primary mouse macrophages. Phagocytosis in the presence of soluble peptides showed cyclic > wildtype > scrambled activity, with the same trend observed with human cells. Opsonized cells that were not engulfed adhered tightly to macrophages, with opposite trends to phagocytosis. Peptide activity is nonetheless higher in human versus mouse assays, consistent with species differences in CD47−SIRP$\alpha$. Small peptides thus function as soluble antagonists of a major macrophage checkpoint.

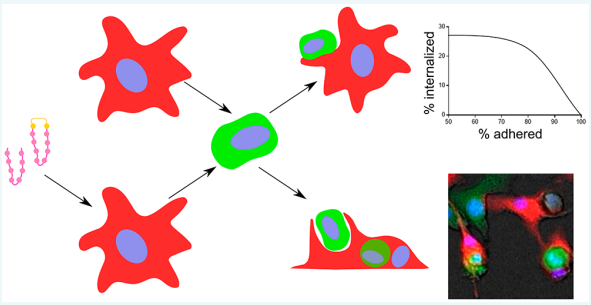


Macrophages engulf a cell or particle based not only on receptor interactions with activating ligands but also on the presence of inhibitory signals, most notably from CD47. This integral membrane protein expressed on all human cells interacts with the macrophage checkpoint receptor SIRP$\alpha$ to inhibit phagocytosis, particularly when phagocytosis is driven by IgG antibodies that bind and activate FcR receptors on macrophage.[1,2] Display of CD47 on nanoparticles and on gene therapy viruses delays their clearance and increases delivery to disease sites,[3,4] complementing methods such as PEGylation that attenuate nonspecific opsonization, especially by IgG.[5,6] CD47-mimetic peptides that bind SIRP$\alpha$ and show similar functionality began with a 21-amino acid "Self" peptide that helped to image and shrink tumors.[3] In parallel, immunotherapeutic efforts focusing on CD47 have led to blocking antibodies that suppress tumors in the clinic if-and-only if combined with phagocytosis-driving interactions, especially tumor-specific IgG.[7] Such efforts and those with particles and implanted materials[8] motivate the development of additional peptides that regulate SIRP$\alpha$ function.

Cyclic peptides are generally attractive because of their enhanced stability against degradation and increased conformational stability.[9] The latter can, in principle, lead to increased specificity of a peptide for its intended receptor and is particularly relevant to probing human versus mouse differences in CD47−SIRP$\alpha$ interactions.[10] Natural cyclic peptides include the toxic mushroom-derived, hepta-peptide phalloidin that binds and stabilizes F-actin,[11] but synthetic cyclic peptides also show specific activity.[9] Cyclic-RGD for example disrupts cell adhesions as a soluble antagonist[12] but also mediates adhesion as a bioconjugate to particles and materials.[13] Here, we synthesize small cyclic human CD47-derived peptides with similar dual use potential. We focus on their function as soluble antagonists of CD47−SIRP$\alpha$ to increase engulfment of IgG-opsonized cells, particularly mouse melanoma cells. The selected cells are a standard preclinical model for solid tumors but also are challenging for anti-CD47 blockade.[14] We have recently demonstrated disruption of the CD47−SIRP$\alpha$ axis with potent linear nano-Self (nS) peptides that promote macrophage phagocytosis of opsonized cancer cells.[15] In this study, the activity of cyclic nano-Self (nS-Cyc) variants that share the same core sequences as their linear counterparts are tested and compared to linear nS peptides. We find that macrophage engulfment of opsonized cells is enhanced in the presence of nS-Cyc peptide with wildtype sequence, particularly compared to the linear form. We also find antagonist function in human cell assays exceeds that with mouse cells, consistent with specificity gains upon cyclization.

**Special Issue:** What Comes after Liposomes? Self-Assembled Systems

**Received:** January 16, 2022
**Revised:** March 9, 2022

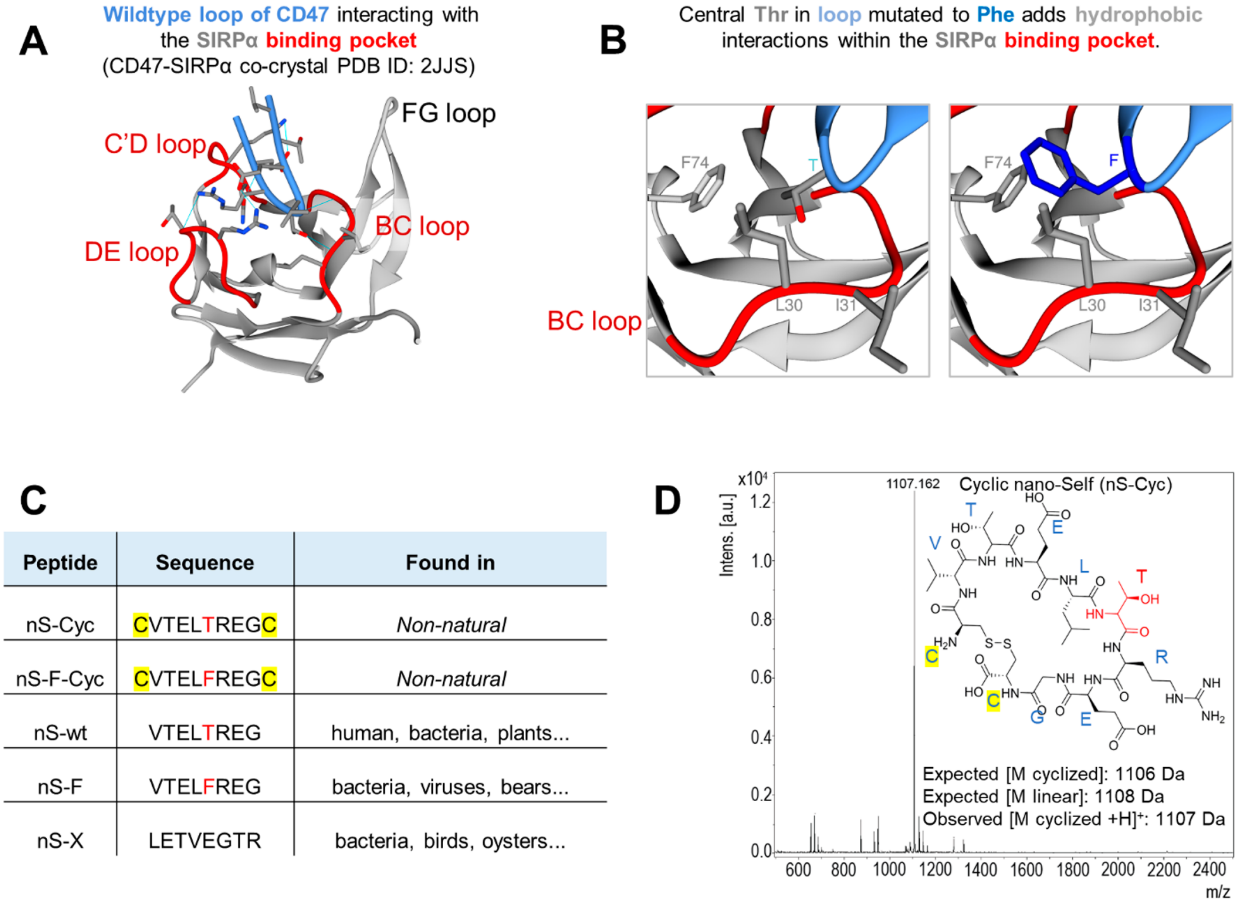


**Figure 1.** Cyclic nano-self-peptides are designed based on the human CD47−SIRP$\alpha$ interaction. (A) Derived from CD47, the 8-amino acid nano-Self-peptide region in CD47 (blue) interacts with 3 (red) out of the 4 loops in SIRP$\alpha$ (gray) that make up the binding pocket which amounts to roughly 40% of all contact residues between the two proteins. PDB: 2JJS. (B) The critical polar Thr residue in nS-wt (blue) is inserted into a hydrophobic core in the SIRP$\alpha$ binding pocket (red). Mutating the polar Thr to a hydrophobic Phe, which can also engage in $\pi$-stacking interactions with Phe[74] away from the SIRP$\alpha$ binding pocket, might enhance binding of the peptide. (C) The sequences of the linear nano-Self-peptides (including the scrambled nS-X sequence) are found in natural organisms, whereas the cyclic variants are not natural. (D) Chemical structure of the cyclic nano-Self-peptide. Synthesis of the cyclic peptide was characterized using MALDI-TOF mass spectrometry.

## RESULTS

**Synthesis and Characterization of Cyclic and Linear Nano-Self-Peptides.** The cocrystal structure of CD47−SIRP$\alpha$ shows the highest density of CD47 contacts localizes to a $\beta$-hairpin loop that docks into a hydrophobic pocket of SIRP$\alpha$ (Figure 1A). Despite additional interactions outside this binding site, we hypothesized that cyclic peptides could be made based on this eight amino acid loop and that the synthetic nS-Cyc peptide would maintain activity. Furthermore, a Thr residue in the center of the $\beta$-hairpin shows multiple contacts with SIRP$\alpha$'s hydrophobic pocket (Figure 1B), leading us to further hypothesize that mutating the Thr to a more hydrophobic Phe residue could strengthen the interactions of nS peptides with SIRP$\alpha$ (Figure 1C). Terminal Cys residues allowed for cyclization via disulfide formation, and a scrambled nS-X peptide was also made as a control. Our particular design of the nS-Cyc excludes two Glu residues that normally flank the eight residue wildtype CD47 sequence (Figure S1). Repulsion of these two negative charges likely undermines binding to SIRP$\alpha$ as observed with a similar cyclic peptide that included these two Glu residues.[3]

Cyclic and linear nS peptides were synthesized on rink amide resins resulting in C-terminal amide groups. This modification also eliminates a negative charge. Matrix-assisted laser desorption ionization-time-of-flight (MALDI-TOF) results proved consistent with the predicted mass-to-charge ratios ($m/z$), and analytical HPLC confirmed >98% peptide purity (Figures 1D and S2).

**nS Peptides Increase Macrophage Phagocytosis of Antibody-Opsonized Cells.** To focus on the possible function of our nS peptides as soluble antagonists of CD47−SIRP$\alpha$, we first tested their effects on the phagocytosis of mouse melanoma B16F10 cells (B16 for brevity) by mouse bone marrow-derived macrophage (BMDM). B16s are a standard model for preclinical immunotherapy,[16,17] but success with anti-CD47 blockade remains a challenge even when combined with IgG-opsonization of B16 to promote phagocytosis.[14] As per the latter study, B16 opsonization was done here with a "mAb", the monoclonal anti-TYRP1 IgG that binds the melanocyte-specific tyrosinase-related protein 1 (TYRP1)[18] for our phagocytosis assay.[19] B16 cells (expressing GFP) were detached from their culture dishes, opsonized with


https://doi.org/10.1021/acs.bioconjchem.2c00020
Bioconjugate Chem. XXXX, XXX, XXX−XXX

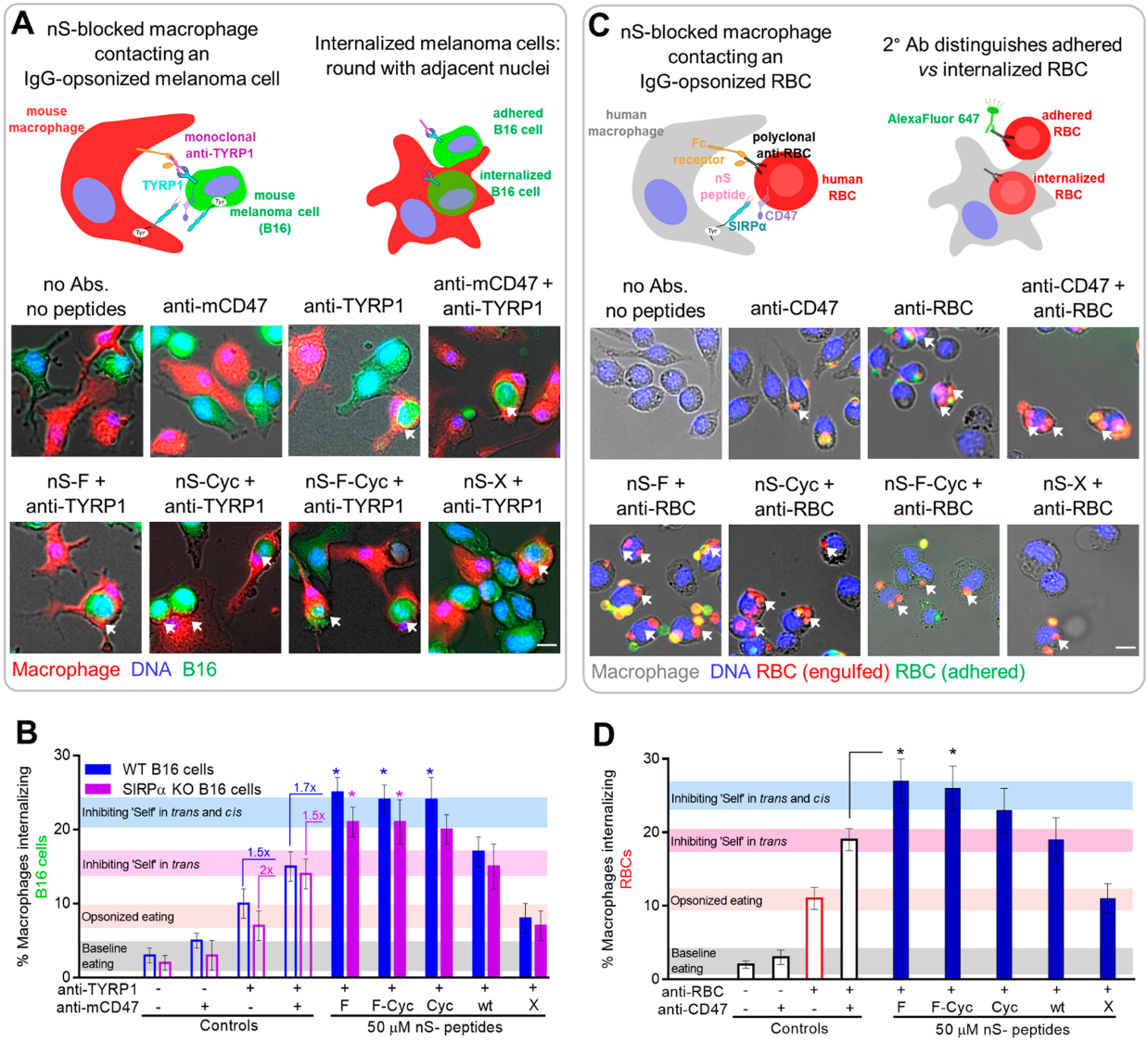


**Figure 2.** Phagocytosis of antibody-opsonized mouse and human target cells is enhanced in the presence of linear and cyclic nano-Self-peptides. (A) SIRP$\alpha$ knockout (KO) or parental (WT) mouse melanoma B16 cells are anti-TYRP1 opsonized and phagocytosed by mouse bone marrow-derived macrophages in the presence of the nano-Self-peptides (top). Internalization of B16 cells (green) is distinguished from adherent cells by the physical rounding up the cells inside the macrophages because B16 cells can attach and spread on plastic (bottom) (scale bar = 25 $\mu$m). (B) Phagocytosis of both WT (blue) and SIRP$\alpha$ KO (purple) B16 cells is enhanced significantly by the linear and cyclic nS-F peptides. nS-wt had similar effects as anti-mCD47 with no effect of nS-X on phagocytosis. *Cis* interactions between CD47 and SIRP$\alpha$ on B16s effects phagocytosis levels with less phagocytic macrophages against SIRP$\alpha$ KO B16s because of more accessible CD47 molecules on their membranes. Hyper-phagocytosis is also observed when BMDMs are treated with potent nS-F and cyclic variants. Control conditions are represented by empty bars. The plus and minus signs indicate the addition or lack of the respective antibodies to the melanoma cells. At least 200 macrophages were analyzed per condition. (* denotes $p < 0.05$ relative to anti-mCD47 and anti-TYRP1 treated B16s.) (C) The *in vitro* phagocytosis of red blood cells is achieved by disrupting the CD47−SIRP$\alpha$ axis with nano-Self-peptides and supplying a strong phagocytic stimulus via macrophage FcR-binding to IgG antibodies (top). Phagocytosed (red) and uninternalized red blood cells (green) are visualized using fluorescence microscopy as seen in the representative overlays (bottom) (scale bar = 25 $\mu$m). (D) Phagocytosis levels are enhanced when macrophages are incubated with saturating concentrations of nano-Self-peptides as does CD47-blockade of red blood cells. Mutating the critical Thr residue to Phe in the linear (nS-F) and cyclic (nS-F-Cyc) variants increases macrophage phagocytosis by roughly 25% relative to nS-wt, while no effect is observed in the presence of scrambled nS-X. Hyper-phagocytosis is observed for F-variants because of simultaneous *cis* and *trans* inhibition of the CD47−SIRP$\alpha$ axis. Control conditions are represented by empty bars. The plus and minus signs indicate the addition or lack of the respective antibodies to the red blood cells. At least 200 macrophages were analyzed per condition. (* denotes $p < 0.05$ relative to anti-CD47 and anti-RBC treated RBCs.)

anti-TYRP1, and then added to well-spread BMDMs that were labeled with red dye and pretreated or not with our various peptides (Figure 2A, top). Microscopy showed internalization, or "eating," of rounded B16s especially when anti-mCD47 or our various nS peptides were also added (Figure 2A, images). Scrambled nS-X peptide was the clear exception. B16s that


https://doi.org/10.1021/acs.bioconjchem.2c00020
Bioconjugate Chem. XXXX, XXX, XXX−XXX

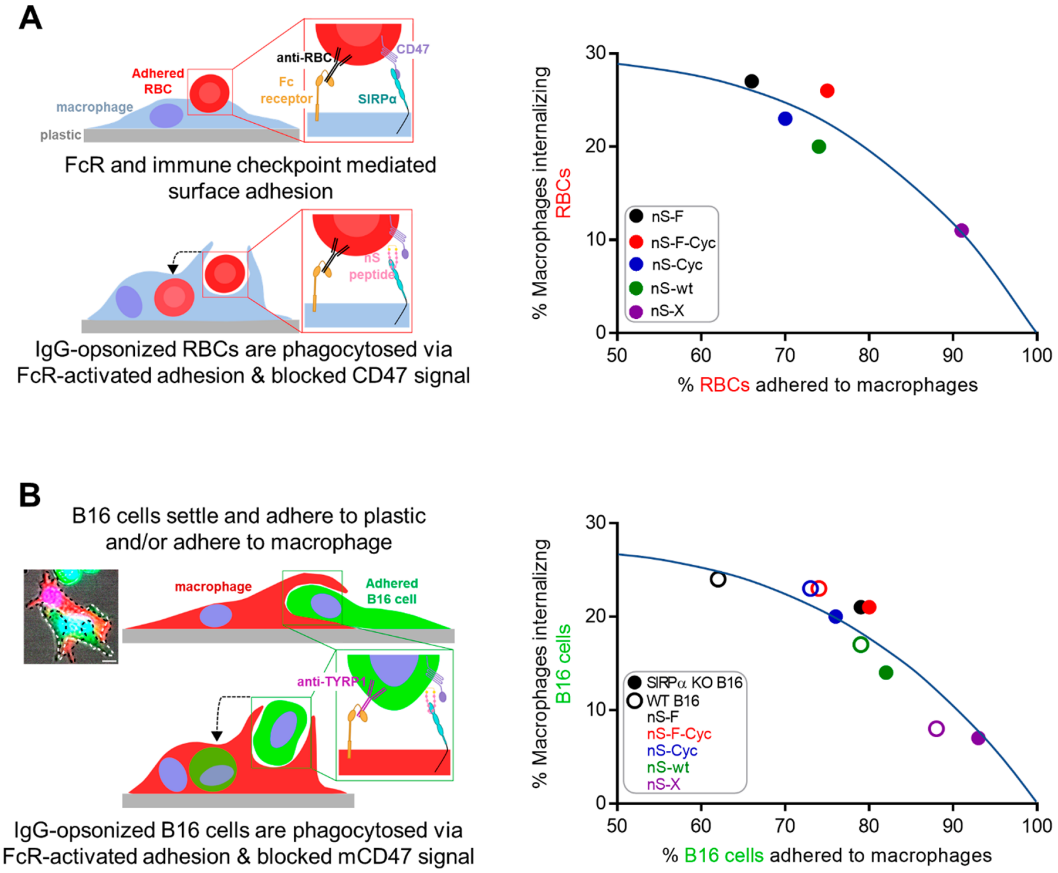


**Figure 3.** nano-Self-peptides minimize target cell adhesion to macrophage leading to increased phagocytosis. (A) Opsonized RBCs adhere to the surface of macrophages through IgG−FcR-mediated binding in addition to possible CD47−SIRP$\alpha$ binding that silences uptake of RBCs. FcR-mediated activation leads to macrophage uptake in the presence of the nS peptides that also effectively block CD47−SIRP$\alpha$ binding. The % Adhered RBCs is measured from the total RBCs imaged, which are either adherent to a macrophage or else internalized. (B) Opsonized B16 cells adhere to macrophages through FcR-binding as well as CD47−SIRP$\alpha$ binding but also compete for the plastic surface. Once attached and spread on plastic, the macrophage cannot strip the cancer cell off. B16 cells that interact with macrophages while in suspension are engulfed when nano-Self-peptides are added. Insert: a BMDM (red fluorescence, black outline) contacting an adhered, opsonized B16 cell (green fluorescence, white outline). Nonlinear regression fits (see text): RBC: $y_{max} = 30$; $m = 4.95$; $A^m = 7.46 \times 10^{13}$; $B^m = 1.37 \times 10^{11}$; $p = 0.03$. B16: $y_{max} = 27.8$; $m = 4.94$; $A^m = 9.26 \times 10^{12}$; $B^m = 4.69 \times 10^{10}$; $p_{WT} = 0.04$; $p_{KO} = 0.02$.

were not engulfed were often attached and spread on the dishes similar to the BMDMs.

Quantitation of the percentage of macrophages that had engulfed opsonized B16s was done for WT B16s as well as SIRP$\alpha$ knockout B16s (KO). Many cell and cancer types express SIRP$\alpha$, including B16 melanoma (Figure S3).[20] KO of SIRP$\alpha$ on B16s removes its *cis* interactions with CD47 on the same cell, allowing for more accessible "don't eat me" signaling by CD47 through *trans* interactions with SIRP$\alpha$ on the opposing macrophage.[19] This assay effectively represents cancers that are CD47-rich and SIRP$\alpha$-negative.

Anti-mCD47 on both B16 lines showed baseline eating [Figure 2B: (−, −) vs (−, +)], whereas anti-TYRP1 consistently showed higher opsonized eating that increased further upon addition of anti-mCD47 [Figure 2B: (+, −) vs (+, +)]. The latter inhibition of CD47 gave similar levels of eating for WT and KO B16s, consistent with equal inhibition of CD47's "Self" interactions in *trans* with SIRP$\alpha$ on macrophages. However, the results also represent 50% and 100% increases, respectively, relative to anti-TYRP1 opsonization alone, consistent with the model that the KO B16 effectively displays more CD47.

Maximum levels of phagocytic macrophages were measured with nS-F, nS-F-Cyc, and nS-Cyc peptides [Figure 2B: (+, nS peptides)], with lower levels for linear nS-wt that are similar to the effects of anti-mCD47 on engulfment of opsonized WT and KO B16s. Scrambled nS-X peptide does not affect opsonization-driven eating of the two B16 lines. The maximum levels of eating with soluble nS-F, nS-F-Cyc, and nS-Cyc are consistent with disruption of both *trans* and *cis* interactions between CD47−SIRP$\alpha$ on the macrophages, per previous studies showing suppression of a basal level of inhibitory "don't eat me" signal;[15,19] nS peptides are unlikely to bind and inhibit SIRP$\alpha$ on WT B16 cells because excess peptide is washed away in our assay before adding B16s to the macrophages. Regardless, the increased phagocytosis follows the trend cyclic > wildtype > scrambled activity, and though the mutant Phe residue makes linear > wildtype, it has no effect on the cyclic peptide.

The above phagocytosis results with mouse cells are somewhat surprising because our nS peptides were designed


https://doi.org/10.1021/acs.bioconjchem.2c00020
Bioconjugate Chem. XXXX, XXX, XXX−XXX

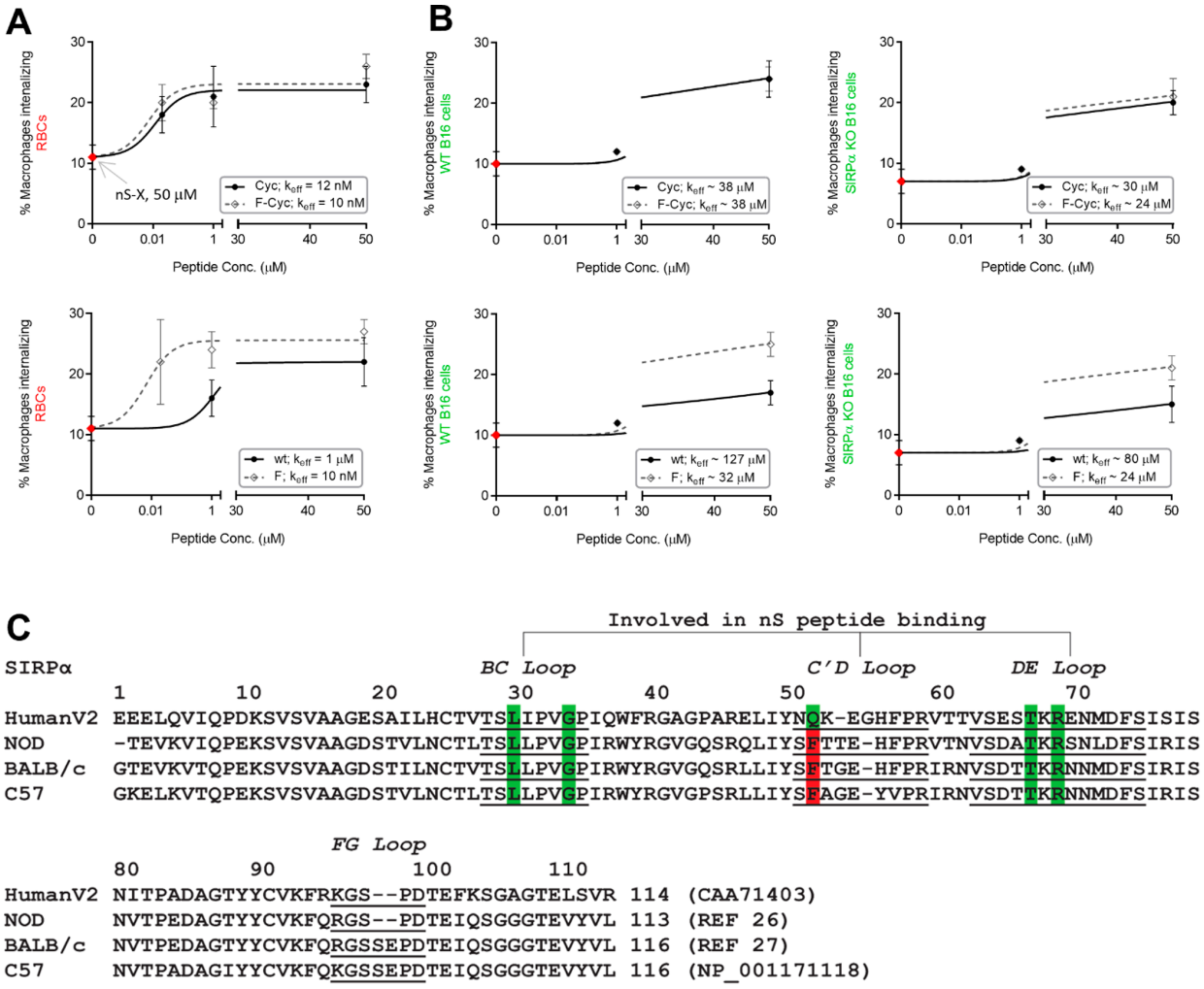


**Figure 4.** Engineered nano-Self-peptides are potent at nanomolar concentrations for human macrophage phagocytosis but much weaker with primary mouse macrophages. (A) Saturating human macrophages with the various nano-Self-peptides results with maximum macrophage internalization of opsonized RBCs. At nanomolar concentrations, the nano-Self-peptide variants are effective at promoting near-maximum macrophage phagocytosis with significantly lower efficacy for nS-wt. (B) Estimates for effective concentrations of the nS peptides function in mouse BMDMs for phagocytosing B16 cells. (C) SIRP$\alpha$ sequence analysis between human and various mouse species reveals significant changes in the binding loop sequences (underlined residues). All highlighted residues are directly involved in binding the nS-wt region of CD47. Green highlighted residues are conserved relative to human SIRP$\alpha$ variant 2. Red highlighted residues are nonconserved mutations disrupting H-binding.

based on the structure of *human* CD47 interacting with *human* SIRP$\alpha$ (Figure 1A,B), and because mouse sequences differ.[3] Phagocytosis assays therefore focused next on a simple human system of fresh human red blood cells (RBCs) and human THP-1 macrophages, as previously studied.[15] RBCs were opsonized with a polyclonal IgG (a rabbit anti-human RBC) and then added to the cultured macrophages that had been nS peptide treated (Figure 2C-Top). RBCs were the cells where CD47's "Marker of Self" function was first identified,[21] but solely blocking CD47 on the RBC does not significantly affect baseline eating, with <5% of macrophages internalizing one or more RBCs [Figure 2D: (−, −) vs (−, +)]. Opsonization more than doubles the extent of phagocytosis, and addition of anti-CD47 doubles again this internalization [Figure 2D: (−, +) vs (+, +)]. The results are consistent with "self" recognition only when coupled to a pro-phagocytic cue.[3]

Maximum levels of phagocytic macrophages were once again measured with peptides nS-F, nS-F-Cyc, and nS-Cyc peptides [Figure 2B: (+, nS peptides)], which aligns well with the mouse results. Lower levels of phagocytosis for linear nS-wt are likewise similar to anti-CD47 effects on engulfment of opsonized RBCs, and scrambled nS-X peptide does not affect opsonization-driven eating of RBCs. The maximum levels of eating with soluble nS-F, nS-F-Cyc, and nS-Cyc are again consistent with disruption of both *trans* and *cis* interactions between CD47−SIRP$\alpha$ on the macrophages. Overall, mouse and human assay results are not only similar in trend but also similar in quantitation with the nS-peptide maxima of ∼25% for phagocytosis of opsonized cells.

**Maximum Phagocytosis Also Minimizes Residual Adhesion to Macrophages.** Opsonized RBCs that contact macrophages will tend to adhere to the macrophages, and any subsequent internalization should in principle lead to a


https://doi.org/10.1021/acs.bioconjchem.2c00020
Bioconjugate Chem. XXXX, XXX, XXX−XXX

decrease in the number of macrophage-adherent RBCs. Importantly, the CD47−SIRP$\alpha$ interaction mediates RBC adhesion,[22] and a peptide such as nS-X that does not seem to affect the CD47−SIRP$\alpha$ interaction (Figure 2B,D) should lead to more residual adhesion than, for example, the nS-Cyc peptide that effectively inhibits CD47−SIRP$\alpha$ while increasing internalization (Figure 3A, sketch).

To measure the residual adhesion of RBCs and distinguish it from internalization by macrophages, our engulfment assay with human RBCs used a secondary antibody against the opsonizing IgG, which allowed us to clearly see RBCs in contact with macrophages that are not internalized (Figure 2C). The cells are also firmly attached to the macrophages because the culture dishes were rinsed after fixation and secondary antibody labeling. Quantitation of the macrophage-adherent RBCs shows a significant anticorrelation with phagocytosis for the nS peptide samples ($p < 0.05$) (Figures 3A plot and S4). All of the RBCs in these samples are equally opsonized with IgG that binds Fc-receptors (FcR's) on macrophages, and so differences in measured adhesion implicate differences in the CD47−SIRP$\alpha$ interaction. Blockade of this immune checkpoint interaction by nS-F and nS-Cyc understandably shows the lowest amount of residual adhesion to macrophages, whereas the inactive nS-X has no effect on phagocytosis of opsonized RBCs (Figure 2D), resulting in predominantly adherent RBCs.

When a melanoma cell suspension is added to a macrophage culture, the melanoma cell can (i) adhere and spread on the plastic culture dish far from a macrophage, (ii) adhere entirely or partially to a macrophage, or else (iii) adhere to a macrophage and be internalized (Figure 2A, images). Note that B16s are typical of adherent cell types and will attach strongly to plastic within 1−2 h, unlike RBCs; likewise *in vivo*, B16s will generally adhere to each other and to other cells and matrix, unlike RBCs in freely flowing blood. Opsonized melanoma cells should nonetheless adhere to any contacting macrophages through both the IgG−FcR interaction and the CD47−SIRP$\alpha$ interaction, although the latter should again be inhibited by the nS peptides that specifically antagonize CD47−SIRP$\alpha$ (Figure 3B, sketch). We defined as macrophage-adherent the opsonized B16s that were not internalized but were in clear contact with a macrophage while also possibly adhering to the plastic dish (Figure 3B, inset image); quantitation of these macrophage-adhered B16s again shows an anticorrelation with phagocytosis for the numerous nS peptide samples ($p < 0.05$) (Figure 3B, plot). The nS peptides that maximized phagocytosis also minimized the macrophage-adhered B16s, consistent with the human RBC results despite the additional means of B16 attachment in these assays. Moreover, the WT B16s adhered less than the corresponding KO B16s, consistent with the greater phagocytosis of the WT B16s.

These human and mouse plots were fit with a suppression model:

$$y = [y_{max} - (A/B)^m] + A^m/(B^m + x^m)$$

Key fit parameters are remarkably similar for both species, with $y_{max} \approx 30\%$, $m \approx 5$, and only ~2-fold differences in $A^m$ and $B^m$ parameters. The finding of a common phagocytosis asymptote $y_{max}$ indicates that for this assay done over a few hours the macrophage cultures are saturating their phagocytic capacity to a similar extent.

**nS Peptides Have Stronger Effects with Human than with Mouse Macrophages.** All of the results above used 50 $\mu$M peptide, which is >50-fold higher than the ~0.1−1 $\mu$M affinity between human CD47 and human SIRP$\alpha$.[3,10] Using lower concentrations in the assays of opsonized human-RBCs being eaten by human macrophages shows not only that 50 $\mu$M has a saturating effect for all of the active peptides (Figure 4A) but also that the effective potency follows trends nS-Cyc ≈ nS-F-Cyc ≈ nS-F > nS-wt > nS-X. The effective potency ($k_{eff}$) of ~1 $\mu$M for nS-wt is weaker than the affinity of CD47−SIRP$\alpha$[3,10] and could reflect the fact that this short peptide lacks the proper loop structure for binding (entropy contribution) and also lacks other contacts that full-length CD47 has with SIRP$\alpha$ (enthalpic contribution). Our finding of $k_{eff} \approx 10$ nM for the cyclic peptides indeed suggests some advantages of a loop conformation. The Phe substitution also adds to the affinity of the linear nS-F relative to nS-wt but evidently does not help or hinder the cyclic peptide. The lower concentrations of active peptides also typically show more RBC adhesion than the saturating 50 $\mu$M (Figure S4), consistent with the expected trend (Figure 3A). Surprisingly, similar dilution studies of the active nS peptides show no activity in the mouse-focused assays of opsonized B16s eaten by primary mouse macrophages—for both WT and KO B16s (Figure 4B). These human-derived sequences are estimated to have much weaker effective activities ($k_{eff} \approx 20-120$ $\mu$M) as antagonists of mouse CD47−SIRP$\alpha$ interactions.

## DISCUSSION

The nano-Self-sequence nS-wt is directly from the *human* CD47 loop that interacts with *human* SIRP$\alpha$ (Figure 1A) and differs from *mouse* CD47 only at the central Thr residue, which is a Ser in mouse. This conservative Thr−Ser mutation applies to the C57 strain of mouse, from which the B16 melanoma cells and macrophages studied here were obtained. It also applies to the BALB/c strain of mouse, for which we have recently shown the linear nS-F peptide is antagonistic toward "self" recognition by J774A.1 macrophages.[15] Antagonistic activity in the mouse melanoma assays (Figures 2B and 3B) by the human wildtype cyclic and linear peptides is thus anticipated. Maximum activities of 25-30% in both the mouse and human assays could reflect the short assay times or other systematic aspects of the measurements rather than the choices of particular cells that range from primary (BMDM and human-RBC) to lines (B16 and THP-1).

Weak effective affinity of all nS peptides in the mouse assays (Figure 4B) seems consistent with other studies of human CD47 interacting with various mouse SIRP$\alpha$.[15,23−25] Two of SIRP$\alpha$'s three binding loops and several contact residues[10] show sequence differences (Figure 4C). One notable difference is a hydrophobic Phe in a mouse loop of SIRP$\alpha$, which in human is a nonconserved Gln and which will tend to interact with the Phe in the nS-F and nS-F-Cyc peptides, thereby competing with hydrophobic interactions deeper in the binding pocket. Indeed, our recent studies of a bivalent nS-FF antagonist greatly increased human macrophage phagocytosis of human erythroleukemia and RBCs, but this bivalent peptide shows reduced activity with mouse macrophages (Figure S5). Sequences and structures of both SIRP$\alpha$ and CD47 are likely to affect binding and activity, consistent with recent analyses of antibodies.[10] Furthermore, outside the binding site, the FG loops of SIRP$\alpha$ in C57 and BALB/c show Ser-102 and Glu-103 are absent in SIRP$\alpha$ of both human and


https://doi.org/10.1021/acs.bioconjchem.2c00020
Bioconjugate Chem. XXXX, XXX, XXX−XXX

NOD mouse strain that binds human CD47 (Figure 4C), and inserting these two amino acids into NOD SIRP$\alpha$ has been shown to weaken human CD47 binding.[23]

Although there are many FDA-approved therapeutic antibodies against various diseases and a few malignancies,[26] many clinical challenges associated with large IgG antibodies persist, including immunogenicity. These include limited tissue penetration, on-target toxicities, high production costs, and relatively low concentrations.[27] Naturally derived and synthetic peptides have potential clinical advantages such as high soluble concentrations, high tissue penetration, high specificity for a target, and minimal accumulation in organs. Challenges include short plasma half-life, low bioavailability, and poor pharmacokinetics.[28] Nevertheless, peptide therapeutics are increasingly being approved:[29,30] among the 17 FDA-approved peptides since 2016, 11 of these peptides are between 3 and 8 amino acids in length, and five are cyclic disulfide peptides.[30] Natural cyclic peptides resist proteolytic degradation and show high activity,[31] which generally supports the pharmaceutical development of cyclic peptides.[32] For CD47−SIRP$\alpha$, peptides have been made to bind CD47 and have shown some antitumor efficacy in mouse models.[16,33−36] Recently, macrocyclic 15-amino acid peptides were screened and engineered to block CD47 binding to SIRP$\alpha$, reportedly functioning as noncompetitive, allosteric inhibitors.[37] The nS peptides are the first to be rationally derived from the CD47 protein and directly target and antagonize the SIRP$\alpha$ binding pocket. SIRP$\alpha$ is more restricted in its expression than CD47, which is expressed on every cell in the body, and so CD47-binding peptides that are systemically infused will first bind RBCs (favoring phagocytosis) and then bind in all accessible tissues. Though not directly tested here, we expect that our cyclic-nS peptides will have enhanced stability *in vivo*, which favors their translation as CD47 antagonists.

Soluble, recombinant, and mutant CD47 and SIRP$\alpha$ proteins can block the macrophage checkpoint as can antibodies even if they lack the Fc domain.[38−42] Such antagonists have been pursued to minimize IgG opsonization of targets that favors FcR-mediated phagocytosis and likely explains the various forms of anemia that result from anti-CD47 infusions in the clinic. Our nS peptides potently and consistently enhance phagocytosis of opsonized human[15] and mouse cancer cells, and they do so as effectively as anti-CD47 inhibition on these target cells. Peptides lack Fc domains, and so phagocytosis is driven solely by the specificity of IgG opsonization.

## CONCLUSION

In conclusion, cyclic nS peptides are potent SIRP$\alpha$ antagonists derived from the CD47 binding loop. The disulfide bridge in nS-F-Cyc is expected to enhance the peptide half-life in serum, but other disulfide mimetics and cyclization methods can and should be pursued to further stabilize the structure.[43] Substitution of the critical, polar Thr to hydrophobic Phe resulted in enhanced potency for both linear and cyclic peptides, demonstrating the significance of the sequence to the mechanism of SIRP$\alpha$ antagonism. Moreover, the weaker peptide activity in mouse macrophages relative to human and the opposite effects of bivalent nS-FF in human and mouse macrophages further underscore sequence complementarity as essential for potent activity. Overall, the development of soluble cyclic peptides that potently enhance phagocytosis motivates engineering of pan-allelic peptides to be used as macrophage immune checkpoint inhibitors.

## EXPERIMENTAL METHODS

**Solid-Phase Peptide Synthesis.** *Standard Peptide Synthesis.* All peptides in this study were synthesized on a Rink Amide MBHA Resin (loading density: 0.33 mmol/g; Novabiochem) on a 100 $\mu$mol scale at room temperature (RT) using 9-fluorenylmethoxycarbonyl (Fmoc) chemistry. The resin was transferred to a solid phase peptide synthesis vessel and swelled in *N*,*N*-dimethylformamide (DMF; Sigma) for 30 min with stirring. Deprotection of the Fmoc group was achieved by using 1 mL of 1% w/v 1-hydroxybenzotriazole (HoBT; EMD Millipore) and 2% v/v 1,8-diazabicyclo[5.4.0]-undec-7-ene (DBU; Acros Organics) in DMF and under stirring for 1 min (repeated three times). Last, resin was then washed thoroughly with DMF. Coupling solutions contained 3 equiv of Fmoc-amino acids (Chem-Impex or Oakwood Chemicals), 2.8 equiv of 1-[bis(dimethylamino)methylene]-1H-1,2,3-triazolo[4,5-*b*]pyridinium 3-oxid hexafluorophosphate (HATU; Oakwood Chemicals), and 6 equiv of *N*,*N*-diisopropylethylamine (DIEA; Sigma)—relative to resin—dissolved in a minimal amount of DMF to cover the resin (1−1.3 mL) and were activated for 5 min at RT prior to addition to resin. Coupling reactions were left to proceed for 1 h. Following each coupling reaction, the resin was drained, washed thoroughly with DMF, deprotected as described above, and washed thoroughly with DMF.

*Peptide Cleavage.* Following the final deprotection of the last Fmoc group (except for fluorescent peptides where the last amino acid contains acid labile Boc protecting group), the resin was washed with DMF twice and then twice more with dichloromethane (DCM; Sigma). A 5 mL cleavage cocktail containing 95% trifluoracetic acid (TFA; Acros Organics), 2.5% $H_2O$, and 2.5% triisopropylsilane (TIPS; Oakwood) was added to the reaction vessel and left to stir for 4 h. A 45 mL portion of cold diethyl ether (Sigma) was then added to the cleavage solution precipitating the peptide. To make sure all peptide precipitated, the ether layer was evaporated by air until ∼10 mL of solution was left; thereafter, an additional 40 mL of cold ether was added. The peptide was collected by centrifugation, resuspended in cold ether, and collected by centrifugation again (repeated three times). Depending on the solubility of the peptide, the ether-washed pellet was dissolved in a mixture of 10−40% acetonitrile (ACN; Sigma) in water.

*Generation of Cyclic Peptides.* Cyclic peptides were prepared by coupling Fmoc-Cyc(trt)−OH as the first and last amino acids. Deprotection of the Fmoc groups was achieved following the same procedure mentioned above. After peptide cleavage and ether precipitation, the peptide pellet was exposed to air to allow for disulfide oxidation.

*Purification and Characterization.* All peptides were purified using preparative reversed-phase high-performance liquid chromatography (HPLC) on an Agilent 1260 Infinity II system using a Phenomenex Luna Omega 5 $\mu$m PS C18 100 Å LC column. Varying gradients of ACN and 0.1% TFA in $H_2O$ were used to separate the respective peptides. The purity of each peptide was checked using an analytical Agilent 1260 Infinity II system using a Phenomenex Luna Omega 5 $\mu$m PS C18 100 Å LC column. Mass spectrometry was performed using a Bruker matrix-assisted laser desorption ionization−time-of-flight (MALDI-TOF) Ultraflex III mass spectrometer and $\alpha$-Cyano-4-hydroxycinnamic acid (CHCA; Sigma) as the


https://doi.org/10.1021/acs.bioconjchem.2c00020
Bioconjugate Chem. XXXX, XXX, XXX−XXX

matrix. Peptides were lyophilized using a Labconco FreeZone Plus 12 Liter Cascade Console Freeze-Dry system.

*UV−Vis Measurements.* UV−vis absorption spectrophotometry was performed using a Jasco V-650 Spectrophotometer and 1 cm path length quartz cells. Lyophilized peptide was dissolved in 100 μL of phosphate-buffered saline pH 7.4 (PBS; Thermo Fischer), and the concentration of each peptide was determined by measuring the absorbance at 205 nm and using a calculated extinction coefficient for each peptide because of the lack of aromatic residues in the peptides.[44,45] For fluorescein-labeled peptides, the lyophilized solid was dissolved in 20 μL of dimethyl sulfoxide (DMSO; Sigma) then diluted to 100 μL with PBS. Peptide concentration was determined by measuring the absorbance at 495 nm.

**Cell Culture.** All cells were purchased from American Type Culture Collection (ATCC). Human-derived THP-1 monocytes and mouse B16F10 melanoma cells were cultured in RPMI 1640 media (Gibco). All media were supplemented with 10% v/v fetal bovine serum (FBS; Sigma) and 1% v/v penicillin/streptomycin (Sigma). THP-1 monocytes were cultured in suspension. Differentiation of THP-1 monocytes to macrophages was achieved by addition of 100 ng/mL phorbol myristate acetate (PMA; Sigma) in media for 2 days (unless stated otherwise) and confirmed by attachment of the macrophages to the bottom of the tissue culture plates.

B16F10 SIRPα knockout cells were prepared as previously described.[19] Briefly, B16F10 parental cells were transduced with lentivirus for expression of Cas9 and single guide RNA against SIRPα (5′-TAATTCTAAGGTCATCTGCG-3′, designed using the Broad Institute's CRISPick, manufactured by Integrated DNA Technologies, and integrated into plasmid by using BsmBI restriction digest). Knockout was confirmed by flow cytometry by using anti-mouse SIRPα (P84, Biolegend) with secondary donkey anti-mouse AlexaFluor 647 (Thermo Fisher).

The plasmids LentiV-Cas9_puro and Lenti_sgRNA_EFS_GFP (Addgene #108100 and 65656, respectively) were gifts from Christopher Vakoc. Lentivirus for delivery was done using HEK 293T cells by co-transfecting them with the desired transfer plamids, pVSVg, and psPAX2 at a 2:2:1 ratio (by mass) using MIrus TransIT (MIR6603) transfection reagent. Viral supernatant was collected 48 h after transfection and added to target cells at a 1:1 volumetric ratio with regular cell culture media. Successfully transduced cells were selected using puromycin at 2 μg/mL.

***In Vitro* Phagocytosis Assays.** *RBCs.* Fresh human RBCs were washed twice with 50 mM EDTA (Thermo Fischer) in Dulbecco's phosphate buffered saline (PBS; Gibco) then twice with 5% FBS in PBS. RBCs were opsonized with 20 μg/mL rabbit anti-human RBC antibody (Rockland) in 5% FBS for 1 h at RT with shaking. For CD47 blocked RBCs, 5 μg/mL of mouse anti-human CD47 (B6H12; BD Biosciences) was added. Thereafter, RBCs were washed with PBS three times and stained with PKH26 dye (1:800 dilution in PBS; Sigma) for 1 h at RT with shaking in the dark. RBCs were washed and resuspended in PBS.

THP-1 monocytes were PMA differentiated in RPMI for 48 h. Macrophages were then washed with RPMI media three times. The macrophages were then incubated with 20 nM, 1 μM, or 50 μM of the nano-Self-peptides for 1 h at 37 °C, 5% $CO_2$, and 95% humidity. Those THP-1s were then washed with RPMI three times.

Opsonized RBCs were added to macrophages at a ratio of 10:1 for 1 h at 37 °C, 5% $CO_2$, and 95% humidity. Macrophages were then washed with RPMI three times. Adherent and uninternalized RBCs were lysed with water for 30 s followed by immediate replacement with RPMI media. To distinguish the remaining adherent RBCs from internalized RBCs, opsonized RBCs were stained with AlexaFluor 647 donkey anti-rabbit (binds to rabbit polyclonal opsonin on RBC; Invitrogen) IgG (1:1000) while unopsonized, and CD47 blocked RBCs were stained with AlexaFluor 647 donkey anti-mouse (binds to mouse monoclonal anti-CD47 on RBCs; Invitrogen) IgG (1:1000) for 30 min. After washing, macrophages were fixed with 4% formaldehyde (Sigma) for 15 min at RT, washed with PBS, stained with 1 μg/mL Hoechst 33342 (Invitrogen), and then washed with PBS again.

*B16F10 Melanoma Cells.* Bone marrow cells were isolated from femurs and tibias of healthy C57BL6/J mice (The Jackson Laboratory) and cultured in 10 cm Petri dishes containing IMDM (Gibco) supplemented with 10% v/v FBS, 1% v/v penicillin/streptomycin, and 1:10,000 macrophage colony stimulating factor cytokine (M-CSF; Biolegend) for 7 days at 37 °C, 5% $CO_2$, and 95% humidity. All animal experiments were performed according to protocols approved by the University of Pennsylvania's IACUC (protocols 805977 and 804455). The resulting mouse bone marrow-derived macrophages (BMDMs) were washed with PBS containing $Ca^{2+}/Mg^{2+}$ (Gibco) then detached with 0.25% trypsin-EDTA (Gibco) and replated in 6-well tissue culture plates using IMDM+M-CSF (1:10,000) for 24 h.

Mouse melanoma B16F10 cells were washed with PBS containing $Ca^{2+}/Mg^{2+}$ and then trypsinized with 0.05% trypsin-EDTA. After being washed twice with PBS, the cells were labeled with 1:10 000 CFDA-SE (Thermo Fisher) in PBS for 10 min. B16F10 cells were washed then opsonized with 10 μg/mL anti-TYRP1 (TA99; Bio X Cell) in PBS for 2 h at 4 °C with occasional inverting. For CD47 blocked B16F10 cells, 5 μg/mL of anti-mouse CD47 (B6H12; BD Biosciences) was added. During the incubation time, the BMDMs were washed with media then stained with 1:2000 CellTracker Deep Red (Thermo Fisher) in PBS with $Ca^{2+}/Mg^{2+}$ for 10 min. After washing, 50 μM of the nano-Self-peptides were incubated with the BMDMs for 1 h at 37 °C, 5% $CO_2$, and 95% humidity. Finally, BMDMs were washed twice with PBS and then twice with serum-free IMDM.

Without removing the supernatant, the opsonized melanoma cells were added to the labeled BMDMs at a ratio of 2:1 for 2 h at 37 °C, 5% $CO_2$, and 95% humidity. During the last 15 min of the assay, the cells were Hoechst stained. The wells were washed with serum-free IMDM, fixed with 4% formaldehyde for 15 min at RT, and PBS washed. Fluorescence imaging was performed using an Olympus IX71 with a digital EMCCD camera (Cascade 512B) and a 40×/0.6 NA objective. Quantification was done with ImageJ (NIH). At least 200 cells were analyzed, and two-tailed student's *t* test was used to determine statistical significance.

## ■ ASSOCIATED CONTENT

### Supporting Information

The Supporting Information is available free of charge at https://pubs.acs.org/doi/10.1021/acs.bioconjchem.2c00020.

Analytical HPLC and chromatograms, MALDI-TOF spectra, flow cytometry analysis, RBC adhesion analysis



https://doi.org/10.1021/acs.bioconjchem.2c00020
Bioconjugate Chem. XXXX, XXX, XXX−XXX

with varying peptide concentrations, and primary mouse macrophage phagocytosis with bivalent peptide (PDF)

## AUTHOR INFORMATION


### Corresponding Author

**Dennis E. Discher** − *Biophysical Engineering Laboratories and Bioengineering Graduate Group, University of Pennsylvania, Philadelphia, Pennsylvania 19104, United States;* orcid.org/0000-0001-6163-2229; Email: discher@seas.upenn.edu

### Authors

**AbdelAziz R. Jalil** − *Biophysical Engineering Laboratories and Department of Chemistry, University of Pennsylvania, Philadelphia, Pennsylvania 19104, United States;* orcid.org/0000-0002-8031-7045

**Jason C. Andrechak** − *Biophysical Engineering Laboratories and Bioengineering Graduate Group, University of Pennsylvania, Philadelphia, Pennsylvania 19104, United States;* orcid.org/0000-0002-6659-9488

**Brandon H. Hayes** − *Biophysical Engineering Laboratories and Bioengineering Graduate Group, University of Pennsylvania, Philadelphia, Pennsylvania 19104, United States*

**David M. Chenoweth** − *Department of Chemistry, University of Pennsylvania, Philadelphia, Pennsylvania 19104, United States;* orcid.org/0000-0002-0819-4669

Complete contact information is available at: https://pubs.acs.org/10.1021/acs.bioconjchem.2c00020


### Author Contributions

A.R.J. and D.E.D. designed the experiments and research, prepared the figures, and wrote the manuscript. J.C.A. harvested and isolated primary mouse bone marrow macrophages used for the phagocytosis analysis and assisted with manuscript revisions. B.H.H. performed gene analysis on mouse B16 melanoma cells and assisted with manuscript revisions. D.M.C. provided laboratory space, and is a coadvisor on the research project.

### Notes

The authors declare the following competing financial interest(s): ARJ and DED declare submission of a US patent application, Multivalent Nano-Self Peptides and Uses Thereof.

## ACKNOWLEDGMENTS

We thank the Chenoweth laboratory for thoughtful discussions and laboratory space for peptide synthesis as well as the Departments of Bioengineering and Chemistry for facilities. We thank Justine Lee, MS for making the SIRP$\alpha$ KO cell line used here. Funding was provided by the National Science Foundation Materials Science and Engineering Center award DMR-1720530 and DMR-1120901, Pennsylvania Department of Health Grant HRFF 4100083101, and National Cancer Institute grants U01CA254886, U54-CA193417, and National Heart Lung and Blood Institute grant R01-HL124106. J.C.A. and B.H.H. were supported under the National Science Foundation Graduate Research Fellowship Program award DGE-1845298.

## REFERENCES


(1) Barclay, A. N.; van den Berg, T. K. The Interaction Between Signal Regulatory Protein Alpha (SIRP alpha) and CD47: Structure, Function, and Therapeutic Target. *Annu. Rev. Immunol.* **2014**, *32*, 25−50.

(2) Hatherley, D.; Harlos, K.; Dunlop, D. C.; Stuart, D. I.; Barclay, A. N. The Structure of the Macrophage Signal Regulatory Protein Alpha (SIRP$\alpha$) Inhibitory Receptor Reveals a Binding Face Reminiscent of That Used by T Cell Receptors. *J. Biol. Chem.* **2007**, *282*, 14567−14575.

(3) Rodriguez, P. L.; Harada, T.; Christian, D. A.; Pantano, D. A.; Tsai, R. K.; Discher, D. E. Minimal "Self" Peptides That Inhibit Phagocytic Clearance and Enhance Delivery of Nanoparticles. *Science* **2013**, *339*, 971−975.

(4) Sosale, N. G.; Ivanovska, I. I.; Tsai, R. K.; Swift, J.; Hsu, J. W.; Alvey, C. M.; Zoltick, P. W.; Discher, D. E. "Marker of Self" CD47 on lentiviral vectors decreases macrophage-mediated clearance and increases delivery to SIRPA-expressing lung carcinoma tumors. *Molecular Therapy-Methods & Clinical Development* **2016**, *3*, 16080.

(5) Owens, D., III; Peppas, N. Opsonization, Biodistribution, and Pharmacokinetics of Polymeric Nanoparticles. *Int. J. Pharm.* **2006**, *307*, 93−102.

(6) Walkey, C. D.; Olsen, J. B.; Guo, H.; Emili, A.; Chan, W. C. W. Nanoparticle Size and Surface Chemistry Determine Serum Protein Adsorption and Macrophage Uptake. *J. Am. Chem. Soc.* **2012**, *134*, 2139−2147.

(7) Advani, R.; Flinn, I.; Popplewell, L.; Forero, A.; Bartlett, N. L.; Ghosh, N.; Kline, J.; Roschewski, M.; LaCasce, A.; Collins, G. P.; et al. CD47 Blockade by Hu5F9-G4 and Rituximab in Non-Hodgkin's Lymphoma. *N. Engl. J. Med.* **2018**, *379*, 1711−1721.

(8) Stachelek, S. J.; Finley, M. J.; Alferiev, I. S.; Wang, F.; Tsai, R. K.; Eckells, E. C.; Tomczyk, N.; Connolly, J. M.; Discher, D. E.; Eckmann, D. M.; et al. The Effect of CD47 Modified Polymer Surfaces on Inflammatory Cell Attachment and Activation. *Biomaterials* **2011**, *32*, 4317−4326.

(9) Choi, J.; Joo, S. H. Recent Trends in Cyclic Peptides as Therapeutic Agents and Biochemical Tools. *Biomolecules & Therapeutics* **2020**, *28*, 18−24.

(10) Jalil, A. R.; Andrechak, J. C.; Discher, D. E. Macrophage Checkpoint Blockade: Results From Initial Clinical Trials, Binding Analyses, and CD47-SIRPa Structure-Function. *Antibody Ther* **2020**, *3*, 80−94.

(11) Wang, S.; Crevenna, A. H.; Ugur, I.; Marion, A.; Antes, I.; Kazmaier, U.; Hoyer, M.; Lamb, D. C.; Gegenfurtner, F.; Kliesmete, Z.; et al. Actin Stabilizing Compounds Show Specific Biological Effects due to their Binding Mode. *Sci. Rep.* **2019**, *9*, 9731.

(12) Hennig, R.; Kuespert, S.; Haunberger, A.; Goepferich, A.; Fuchshofer, R. Cyclic RGD Peptides Target Human Trabecular Meshwork Cells while Ameliorating Connective Tissue Growth Factor-Induced Fibrosis. *J. Drug Target.* **2016**, *24*, 952−959.

(13) Battistini, L.; Bugatti, K.; Sartori, A.; Curti, C.; Zanardi, F. RGD Peptide-Drug Conjugates as Effective Dual Targeting Platforms: Recent Advances. *Eur. J. Org. Chem.* **2021**, *2021*, 2506−2528.

(14) Sockolosky, J. T.; Dougan, M.; Ingram, J. R.; Ho, C. C. M.; Kauke, M. J.; Almo, S. C.; Ploegh, H. L.; Garcia, K. C. Durable Antitumor Responses to CD47 Blockade Require Adaptive Immune Stimulation. *Proc. Natl. Acad. Sci. U. S. A.* **2016**, *113*, E2646−E2654.

(15) Jalil, A. R.; Hayes, B. H.; Andrechak, J. C.; Xia, Y. T.; Chenoweth, D. M.; Discher, D. E. Multivalent, Soluble Nano-Self Peptides Increase Phagocytosis of Antibody-Opsonized Targets while Suppressing "Self" Signaling. *ACS Nano* **2020**, *14*, 15083−15093.

(16) Wang, H.; Sun, Y.; Zhou, X.; Chen, C.; Jiao, L.; Li, W.; Gou, S.; Li, Y.; Du, J.; Chen, G.; et al. CD47/SIRP Alpha Blocking Peptide Identification and Synergistic Effect with Irradiation for Cancer Immunotherapy. *Journal for Immunotherapy of Cancer* **2020**, *8*, No. e000905.

(17) Anderson, K. L.; Snyder, K. M.; Ito, D.; Lins, D. C.; Mills, L. J.; Weiskopf, K.; Ring, N. G.; Ring, A. M.; Shimizu, Y.; Mescher, M. F.; et al. Evolutionarily Conserved Resistance to Phagocytosis Observed in Melanoma Cells is Insensitive to Upregulation of Pro-Phagocytic Signals and to CD47 Blockade. *Melanoma Res.* **2020**, *30*, 147−158.

(18) Vijayasaradhi, S.; Bouchard, B.; Houghton, A. The Melanoma Antigen Gp75 is the Human Homolog of the Mouse-B (Brown) Locus Gene-Product. *J. Exp. Med.* **1990**, *171*, 1375−1380.
(19) Hayes, B. H.; Tsai, R. K.; Dooling, L. J.; Kadu, S.; Lee, J. Y.; Pantano, D.; Rodriguez, P. L.; Subramanian, S.; Shin, J.; Discher, D. E. Macrophages Eat More After Disruption of Cis Interactions between CD47 and the Checkpoint Receptor SIRPa. *J. Cell. Sci.* **2020**, jcs237800.
(20) *Human Protein Atlas Expression of SIRPA in cancer*. https://www.proteinatlas.org/ENSG00000198053-SIRPA/pathology (accessed 8/9/2021).
(21) Oldenborg, P.; Zheleznyak, A.; Fang, Y.; Lagenaur, C.; Gresham, H.; Lindberg, F. Role of CD47 as a Marker of Self on Red Blood Cells. *Science* **2000**, *288*, 2051−2054.
(22) Subramanian, S.; Parthasarathy, R.; Sen, S.; Boder, E.; Discher, D. Species- and Cell Type-Specific Interactions between CD47 and Human SIRP Alpha. *Blood* **2006**, *107*, 2548−2556.
(23) Kwong, L. S.; Brown, M. H.; Barclay, A. N.; Hatherley, D. Signal-Regulatory Protein Alpha from the NOD Mouse Binds Human CD47 with an Exceptionally High Affinity - Implications for Engraftment of Human Cells. *Immunology* **2014**, *143*, 61−67.
(24) Iwamoto, C.; Takenaka, K.; Urata, S.; Yamauchi, T.; Shima, T.; Kuriyama, T.; Daitoku, S.; Saito, Y.; Miyamoto, T.; Iwasaki, H.; et al. The BALB/c-Specific Polymorphic SIRPA Enhances its Affinity for Human CD47, Inhibiting Phagocytosis Against Human Cells to Promote Xenogeneic Engraftment. *Exp. Hematol.* **2014**, *42*, 163−171.
(25) Andreu, N.; Phelan, J.; de Sessions, P. F.; Cliff, J. M.; Clark, T. G.; Hibberd, M. L. Primary Macrophages and J774 Cells Respond Differently to Infection with Mycobacterium Tuberculosis. *Sci. Rep.* **2017**, *7*, 42225.
(26) Kaplon, H.; Reichert, J. M. Antibodies to Watch in 2021. *mAbs* **2021**, *13*, 1860476.
(27) Chames, P.; Van Regenmortel, M.; Weiss, E.; Baty, D. Therapeutic Antibodies: Successes, Limitations and Hopes for the Future. *Br. J. Pharmacol.* **2009**, *157*, 220−233.
(28) Di, L. Strategic Approaches to Optimizing Peptide ADME Properties. *AAPS Journal* **2015**, *17*, 134−143.
(29) Usmani, S. S.; Bedi, G.; Samuel, J. S.; Singh, S.; Kalra, S.; Kumar, P.; Ahuja, A. A.; Sharma, M.; Gautam, A.; Raghava, G. P. S. THPdb: Database of FDA-Approved Peptide and Protein Therapeutics. *PLoS One* **2017**, *12*, No. e0181748.
(30) Al Musaimi, O.; Al Shaer, D.; Albericio, F.; de la Torre, B. 2020 FDA TIDES (Peptides and Oligonucleotides) Harvest. *Pharmaceuticals (Basel, Switzerland)* **2021**, *14*, 145.
(31) Ortega, M. A.; Van Der Donk, W. A. New Insights into the Biosynthetic Logic of Ribosomally Synthesized and Post-translationally Modified Peptide Natural Products. *Cell Chemical Biology* **2016**, *23*, 31−44.
(32) Brayden, D. J.; Hill, T. A.; Fairlie, D. P.; Maher, S.; Mrsny, R. J. Systemic Delivery of Peptides by the Oral Route: Formulation and Medicinal Chemistry Approaches. *Adv. Drug Delivery Rev.* **2020**, *157*, 2−36.
(33) Martinez-Torres, A.; Quiney, C.; Attout, T.; Boullet, H.; Herbi, L.; Vela, L.; Barbier, S.; Chateau, D.; Chapiro, E.; Nguyen-Khac, F.; et al. CD47 Agonist Peptides Induce Programmed Cell Death in Refractory Chronic Lymphocytic Leukemia B Cells via PLC gamma 1 Activation: Evidence from Mice and Humans. *Plos Medicine* **2015**, *12*, No. e1001796.
(34) Martinez-Torres, A. C.; Calvillo-Rodriguez, K. M.; Uscanga-Palomeque, A. C.; Gomez-Morales, L.; Mendoza-Reveles, R.; Caballero-Hernandez, D.; Karoyan, P.; Rodriguez-Padilla, C. PKHB1 Tumor Cell Lysate Induces Antitumor Immune System Stimulation and Tumor Regression in Syngeneic Mice with Tumoral T Lymphoblasts. *Journal of Oncology* **2019**, *2019*, 9852361.
(35) Uscanga-Palomeque, A. C.; Calvillo-Rodriguez, K. M.; Gomez-Morales, L.; Larde, E.; Denefle, T.; Caballero-Hernandez, D.; Merle-Beral, H.; Susin, S. A.; Karoyan, P.; Martinez-Torres, A. C.; et al. CD47 Agonist Peptide PKHB1 Induces Immunogenic Cell Death in T-Cell Acute Lymphoblastic Leukemia Cells. *Cancer Science* **2019**, *110*, 256−268.
(36) Liu, Y.; O'Connor, M.; Mandell, K.; Zen, K.; Ullrich, A.; Buhring, H.; Parkos, C. Peptide-Mediated Inhibition of Neutrophil Transmigration by Blocking CD47 Interactions with Signal Regulatory Protein Alpha. *J. Immunol.* **2004**, *172*, 2578−2585.
(37) Hazama, D.; Yin, Y.; Murata, Y.; Matsuda, M.; Okamoto, T.; Tanaka, D.; Terasaka, N.; Zhao, J.; Sakamoto, M.; Kakuchi, Y.; et al. Macrocyclic Peptide-Mediated Blockade of the CD47-SIRP Alpha Interaction as a Potential Cancer Immunotherapy. *Cell Chemical Biology* **2020**, *27*, 1181.
(38) Ho, C. C. M.; Guo, N.; Sockolosky, J. T.; Ring, A. M.; Weiskopf, K.; Ozkan, E.; Mori, Y.; Weissman, I. L.; Garcia, K. C. "Velcro" Engineering of High Affinity CD47 Ectodomain as Signal Regulatory Protein Alpha (SIRP Alpha) Antagonists that Enhance Antibody-Dependent Cellular Phagocytosis. *J. Biol. Chem.* **2015**, *290*, 12650−12663.
(39) Lee, W. Y.; Weber, D. A.; Laur, O.; Stowell, S. R.; Mccall, I.; Andargachew, R.; Cummings, R. D.; Parkos, C. A. The Role of Cis Dimerization of Signal Regulatory Protein Alpha (SIRP Alpha) in Binding to CD47. *J. Biol. Chem.* **2010**, *285*, 37953−37963.
(40) Lin, Y.; Yan, X.; Yang, F.; Yang, X.; Jiang, X.; Zhao, X.; Zhu, B.; Liu, L.; Qin, H.; Liang, Y.; et al. Soluble Extracellular Domains of Human SIRP Alpha and CD47 Expressed in Escherichia Coli Enhances the Phagocytosis of Leukemia Cells by Macrophages *in Vitro*. *Protein Expr. Purif.* **2012**, *85*, 109−116.
(41) Weiskopf, K.; Ring, A. M.; Ho, C. C. M.; Volkmer, J.; Levin, A. M.; Volkmer, A. K.; Ozkan, E.; Fernhoff, N. B.; van de Rijn, M.; Weissman, I. L.; et al. Engineered SIRP Alpha Variants as Immunotherapeutic Adjuvants to Anticancer Antibodies. *Science* **2013**, *341*, 88−91.
(42) Veillette, A.; Chen, J. SIRP alpha-CD47 Immune Checkpoint Blockade in Anticancer Therapy. *Trends Immunol* **2018**, *39*, 173−184.
(43) Muttenthaler, M.; Andersson, A.; De Araujo, A. D.; Dekan, Z.; Lewis, R. J.; Alewood, P. F. Modulating Oxytocin Activity and Plasma Stability by Disulfide Bond Engineering. *J. Med. Chem.* **2010**, *53*, 8585−8596.
(44) Anthis, N. J.; Clore, G. M. Sequence-Specific Determination of Protein and Peptide Concentrations by Absorbance at 205 nm. *Protein Sci.* **2013**, *22*, 851−858.
(45) Goldfarb, A.; Saidel, L.; Mosovich, E. The Ultraviolet Absorption Spectra of Proteins. *J. Biol. Chem.* **1951**, *193*, 397−404.


https://doi.org/10.1021/acs.bioconjchem.2c00020
*Bioconjugate Chem.* XXXX, XXX, XXX−XXX